


ORIGINAL ARTICLE

The histone demethylase *Utx* controls CD8⁺ T-cell-dependent antitumor immunity via epigenetic regulation of the effector function

Haruna Noda^{1,2,3} | Junpei Suzuki³ | Yuko Matsuoka⁴ | Akira Matsumoto⁵ |
Makoto Kuwahara³ | Yoshiaki Kamei^{1,2} | Yasutsugu Takada² | Masakatsu Yamashita^{3,5} 

¹Breast Center, Ehime University Hospital, Toon, Japan

²Department of Hepato-Biliary-Pancreatic Surgery and Breast Surgery, Graduate School of Medicine, Ehime University, Toon, Japan

³Department of Immunology, Graduate School of Medicine, Ehime University, Toon, Japan

⁴Department of Translational Research Center, Ehime University Hospital, Toon, Japan

⁵Department of Infections and Host Defenses, Graduate School of Medicine, Ehime University, Toon, Japan

Correspondence

Masakatsu Yamashita, Department of Immunology, Graduate School of Medicine, Ehime University, 454 Shitsukawa, Toon City, Ehime, 791-0295, Japan
Email: yamamasa@m.ehime-u.ac.jp

Funding information

Japan Society for the Promotion of Science, Grant/Award Number: KAKENHI/20H03504, KAKENHI/22K07121 and KAKENHI/22K15609

Abstract

CD8⁺ T cells play a central role in antitumor immune responses. Epigenetic gene regulation is essential to acquire the effector function of CD8⁺ T cells. However, the role of *Utx*, a demethylase of histone H3K27, in antitumor immunity remains unclear. In this study, we examined the roles of *Utx* in effector CD8⁺ T-cell differentiation and the antitumor immune response. In a murine tumor-bearing model, an increased tumor size and decreased survival rate were observed in T-cell-specific *Utx* KO (*Utx* KO) mice compared with wild-type (WT) mice. The number of CD8⁺ T cells in tumor-infiltrating lymphocytes (TILs) was significantly decreased in *Utx* KO mice. We found that the acquisition of effector function was delayed and attenuated in *Utx* KO CD8⁺ T cells. RNA sequencing revealed that the expression of effector signature genes was decreased in *Utx* KO effector CD8⁺ T cells, while the expression of naïve or memory signature genes was increased. Furthermore, the expression of *Cxcr3*, which is required for the migration of effector CD8⁺ T cells to tumor sites, was substantially decreased in *Utx* KO CD8⁺ T cells. These findings suggest that *Utx* promotes CD8⁺ T-cell-dependent antitumor immune responses partially through epigenetic regulation of the effector function.

KEYWORDS

antitumor immunity, CD8⁺ T cell, *Cxcr3*, histone H3K27, *Utx*

1 | INTRODUCTION

The role of the immune system in tumor elimination has long been studied in mice, but the existence of an immune response against human tumors has not been clarified. The observation of tumor regression following IL-2 administration and the identification of cancer antigens have promoted research on tumor immunity.¹

Recently, it was shown that the suppression of the immune system at the tumor site is due in part to the interaction between the inhibitory receptor PD-1 expressed on cytotoxic T cells and its ligand PD-L1 expressed on tumor cells.² Suppression of the cytotoxic T-cell function via inhibitory receptors, such as the PD-1/PD-L1 interaction, named the T-cell immune checkpoint, has been shown to play an important role in the immune escape of cancer cells and

Abbreviations: GzmB, granzyme B; IFN- γ , interferon- γ ; OVA, ovalbumin; PD-1, programmed death-1; PD-L1, programmed cell death 1- ligand 1; TCR, T-cell receptor; Th1, type 1, helper T cell; TIL-CD8⁺ T cells, tumor-infiltrating CD8⁺ T lymphocytes; TNF- α , tumor necrosis factor- α .

This is an open access article under the terms of the [Creative Commons Attribution-NonCommercial](https://creativecommons.org/licenses/by-nc/4.0/) License, which permits use, distribution and reproduction in any medium, provided the original work is properly cited and is not used for commercial purposes.

© 2023 The Authors. *Cancer Science* published by John Wiley & Sons Australia, Ltd on behalf of Japanese Cancer Association.

subsequent tumorigenesis.³ Based on this concept, many studies have been conducted to develop immune checkpoint inhibitors that disable the immune evasion system and reactivate cytotoxic T cells by inhibiting the interaction between PD-1 and PD-L1. Indeed, immune checkpoint inhibitors have shown high therapeutic efficacy in small-cell lung cancer, hepatocellular carcinoma, and triple-negative breast cancer, among other lesions.^{4–6}

Naïve CD8⁺ T cells are activated by antigen recognition, acquire effector functions, differentiate into cytotoxic (effector) CD8⁺ T cells, and migrate to the tumor site, playing a critical role in anti-tumor immunity. For cytotoxic T cells to be activated in secondary lymphoid tissues, such as lymph nodes, and migrate to the tumor site, increased expression of chemokine receptors, including CXCR3 and CCR5, and decreased expression of CCR7 are required.^{7–9} The increased expression of adhesion molecules, such as LFA-1, and a decrease in CD62L are also required.^{10,11} Among these molecules, CXCR3 is considered a chemokine receptor essential for the migration of cytotoxic T cells to the tumor site.¹² However, the mechanism underlying the induction of CXCR3 expression upon activation of naïve CD8⁺ T cells remains unclear.

After activation by antigen recognition, naïve CD8⁺ T cells expand clonally and differentiate into effector CD8⁺ T cells, memory CD8⁺ T cells, exhausted CD8⁺ T cells, and senescent CD8⁺ T cells.¹³ The fate of CD8⁺ T cells after antigen recognition is thought to be epigenetically regulated.¹⁴ Epigenetics is the mechanism of acquired regulation of gene expression through modifications of DNA (e.g., methylation) and histones (e.g. methylation, acetylation, phosphorylation, and ubiquitination).^{15,16} It has been well established that chemical modification of histone H3K27 is closely related to enhancer activity.^{17,18} That is, inactive enhancer regions have methylated histone H3K27, whereas activating enhancers have acetylated H3K27. The methylation status of histone H3K27 in mammals is regulated by the methyltransferase Kmt6 (Ezh2) and the demethylases Kdm6a (Utx) and Kdm6b (Jmjd3). Ezh2 reportedly promotes effector CD8⁺ T-cell differentiation and inhibits memory CD8⁺ T-cell formation.¹⁹ In sharp contrast, our group found that Utx, but not Jmjd3, negatively regulates memory CD8⁺ T-cell differentiation.²⁰ Furthermore, Sugata et al. reported that Jmjd3 and Utx play important roles in T-cell differentiation and other processes in the thymus.²¹ However, the role of histone demethylation in CD8⁺ T-cell-dependent antitumor immunity is unclear.

In the present study, we explored the role of Utx in T cells, focusing on the regulation of effector CD8⁺ T-cell-dependent antitumor immunity.

2 | MATERIALS AND METHODS

2.1 | Mice

C57BL6 mice were purchased from Clea Japan, Inc. and used as wild-type (WT) controls in all experiments. *Cd4-Cre* transgenic (Tg) mice and OT-1 Tg mice were purchased from the Jackson Laboratory. *Utx*^{flox/flox} mice and *Jmjd3*^{flox/flox} mice were provided by Dr. Y. Imai

(Ehime University, Ehime, Japan) and Dr. H. Honda (Tokyo Women's Medical University, Tokyo, Japan), respectively. *Ezh2*^{flox/flox} mice (RBRC0555 B6-Ezh2 floxed) were developed by Dr. H. Koseki (RIKEN IMS, Kanagawa, Japan) and Dr. J. Shinga (RIKEN IMS)^{22,23} and provided by the RIKEN BRC through the National Bio-Resource Project of the MEXT. The floxed mice were crossed with *Cd4-Cre* Tg mice to generate T-cell-specific gene-deficient mice. In addition, we generated *Utx* KO OT-1 Tg mice by crossing *Utx* KO mice with OT-1 Tg mice for an in vitro killing assay. Female mice were used at 7–12 weeks old in the experiments.

2.2 | CD8⁺ T-cell stimulation and differentiation in vitro

Naïve CD8⁺ T cells were purified from the spleens of WT mice, *Utx* KO mice, WT OT-1 Tg mice, or *Utx* KO OT-1 Tg mice using a MojoSort CD8⁺ T Cell Isolation Kit (cat# 480035; BioLegend) with biotin anti-CD44 mAb (cat#103004; BioLegend). The cells (7.5×10^5 cells) were then stimulated with immobilized anti-TCR- β mAb (3 μ g/mL, H57-597; BioLegend) and anti-CD28 mAb (1 μ g/mL, 37.5; BioLegend) with IL-2 (10 ng/mL; cat#575406; BioLegend) for 2 days. The cells were then transferred to a new plate and further cultured with IL-2 (10 ng/mL) for the indicated days.

2.3 | Inoculation of tumor cell lines

EL4 thymoma cells, OVA-expressing E.G7 cells (EL4-derivative) and B16 cells were obtained from the ATCC (cat# TIB-39, CRL-2113 and B16-F10, respectively; ATCC). To generate a tumor-carrying mouse model, C57BL/6 mice and T-cell-specific gene-deficient mice were subcutaneously (s.c.) inoculated with E.G7 (5×10^5 cells), EL4 (3×10^6 cells) or B16 melanoma cells (3×10^5 cells) in the lateral flank. Tumor volumes were calculated using the following formula: tumor volume (mm^3) = (short diameter)² \times long diameter/2. For the survival analysis, mice were sacrificed and counted as dead upon reaching a tumor volume of 2000 mm^3 .

2.4 | Flow cytometry

Detailed descriptions are shown in Appendix S1.

2.5 | An enzyme-linked immunosorbent assay (ELISA)

The cells were stimulated with an immobilized anti-TCR- β mAb (3 μ g/mL) for 16 h. The concentrations of IFN- γ and IL-2 in the supernatants were determined using ELISA, as previously described.²⁴ The concentrations of TNF- α were determined using DuoSet ELISA kits (R&D Systems), in accordance with the manufacturer's instructions.

2.6 | Killing assay of activated CD8⁺ T cells

For the in vitro killing assay, the E.G7 target cells and EL4 control cells were labeled with 0.1 and 1 μM Cell Proliferation Dye eFluor 670, respectively. WT and *Utx* KO OT-1 CD8⁺ T cells were cocultured with a 1:1 mixture of E.G7 and EL4 cells in a 96-well U-bottom plate for 6 h. The ratio of E.G7 and EL4 cells was analyzed by flow cytometry. Specific lysis by CD8⁺ T cells was calculated at different ratios of effector and target cells (E:T ratio) using the following formula: specific lysis (%) = (%EL4 cells - %E.G7 cells) / %EL4 cells × 100.

2.7 | Library preparation for RNA-seq

Total RNA was extracted from WT and *Utx* KO CD8⁺ T cells using an RNeasy Plus Micro Kit (Qiagen). Purified RNA samples were prepared for cDNA libraries using the QuantSeq 3' mRNA-Seq Library Prep Kit for Illumina (LEXOGEN). Sequencing of the samples was performed on a NextSeq500 instrument (Illumina) using a NextSeq 500/550 High Output Kit v2.5 (single reads 75 bp).

2.8 | RNA-seq analyses

CLC Genomics workbench 22.0 (Qiagen) was used to trim single reads and align them to the mm10/GRCm38 mouse reference genome. Gene expression was determined by the score of transcripts per million (TPM) mapped reads. The data were deposited in the GSE214673 database. The gene expression data were subsequently subjected to a differentially expressed gene (DEG) analysis using CLC Genomics workbench. DEGs with a fold-change (FC) >2 or <-2 and a false discovery rate (FDR) <0.05 were subjected to functional analyses using Metascape for Gene Ontology (GO) biological process enrichment analysis²⁵ and Heatmapper for visualizing the data.²⁶ Gene set enrichment analysis (GSEA) was performed using the GSEA software program, version 4.2.3.^{27,28} Detailed descriptions of the gene sets are shown in Appendix S1.

2.9 | Quantitative reverse transcriptase PCR (qRT-PCR)

Total RNA was isolated using TRI Reagent (cat#TR118; MOR), and complementary DNA (cDNA) was synthesized using the superscript VILO cDNA synthesis kit (cat# 11754; Thermo Fisher Scientific). qRT-PCR was performed using the Step One Plus Real-Time PCR System (Thermo Fisher Scientific). Primers for qRT-PCR were as follows: Eomes: TaqMan Gene Assay Probe #Mm01351985_m1 (ABI); Lef1: TaqMan Gene Assay Probe #Mm00550265_m1 (ABI); Bach2: 5'-TTCTGGGAAGGTCTGTGAT-3' (forward), 5'-CAGTGAGTCGTGTCCTGTGC-3' (reverse), probe #79; Bcl6: 5'-CTGCAGATGGAGCATGTTGT-3' (forward), 5'-GCCATTTCTGCTTCACTGG-3' (reverse), probe #4; Gzmb: 5'-TGGGAATGCATTTTACCAT-3' (forward),

5'-GCTGCTACTGTGAAGGAAGT-3' (reverse), probe #2; Id2: 5'-AGCTCAGAAGGGAATTCAGATG-3' (forward), 5'-GACAGAACCAGCGTCCA-3' (reverse), probe #89; Id3: 5'-GAGGAGCTTTTGCCACTGAC-3' (forward), 5'-GCTCATCCATGCCCTCAG-3' (reverse), probe #19; Prf1: 5'-CATGTTTGCCTCTGGCCTA-3' (forward), 5'-AATATCAATAACGACTGGCGTGT-3' (reverse), probe #42; Sox4: 5'-CGTCTTGAACCTCGTCGTC-3' (forward), 5'-CTCGTCTCCTCGTCTCT-3' (reverse), probe #63; Tbx21: 5'-AAACATCCTGTAATGGCTTGTG-3' (forward), 5'-TCAACCAGCACCAGACAGAG-3' (reverse), probe #19; and 18s rRNA: 5'-GCAATTATCCCATGAACG-3' (forward), 5'-GGGACTTAATCAACGCAAGC-3' (reverse), probe #48.

2.10 | ChIP assay

Detailed descriptions are shown in Appendix S1.

2.11 | *Listeria* infection for antigen-specific CD8⁺ T-cell response

To assess the antigen-specific CD8⁺ T-cell response, WT or *Utx* KO mice were infected with a recombinant OVA-expressing *Listeria monocytogenes* (*Lm*-OVA) strain (5 × 10³ CFU, intravenous [i.v.]), as previously described.²⁹ The donor cells were prepared and analyzed on day 7 after infection.

2.12 | Statistical analyses

The results were statistically analyzed using a two-tailed unpaired *t*-test. Data are presented as the mean with the standard deviation (SD), as indicated in the figure legends. The survival rate was analyzed according to the Kaplan–Meier actuarial method, with statistical significance determined by the log-rank statistic using JMP software ver.14.1 (SAS Institute). *p*-values <0.05 were considered to indicate statistical significance.

3 | RESULTS

3.1 | Reduced numbers of tumor-infiltrating CD8⁺ T cells and antitumor activity in T-cell-specific *Utx* knockout (KO) mice compared with WT

To clarify the role of histone H3K27 demethylase in the T-cell-dependent antitumor response, we generated mice lacking *Utx* or *Jmjd3* specifically in T cells (*Utx* and *Jmjd3* KO mice, respectively). E.G7-OVA cells, a thymoma cell line expressing OVA as a pseudocarcinoma antigen, were inoculated under the back skin of WT control mice or *Utx* KO mice, and the tumor size was measured over time (Figure 1A). As shown in Figure 1B, tumor sizes were significantly increased in *Utx* KO mice compared with WT mice. The survival ratio

was also significantly reduced in *Utx* KO mice in comparison with WT mice (Figure 1C). Furthermore, similar results were obtained with *Utx* KO mice inoculated with EL4 thymoma or B16 melanoma cells that did not express OVA (Figure 1D–G). In contrast, although the tumor sizes were increased slightly in *Jmjd3* KO mice compared with WT mice, no significant difference in the survival ratio was observed (Figure S1). Therefore, we performed the subsequent analysis using *Utx* KO mice.

A flow cytometric analysis of TILs in mice 14 days after E.G7-OVA inoculation (Figure 2A) revealed that the percentage and number of CD8⁺ T cells were significantly lower in *Utx* KO mice than in WT mice (Figure 2B,C). In contrast, the numbers of total TILs and CD4⁺ T cells were moderately decreased in *Utx* KO mice compared with WT mice, with no statistically significant differences identified (Figure 2C). The percentage of CD8⁺ T cells in the spleen and dLN of the mice 12 days after inoculation with E.G7-OVA was significantly increased in *Utx* KO mice compared with WT mice (Figure 2D). Conversely, the percentage of IFN- γ -positive CD8⁺ T cells was

significantly decreased in tumor-bearing *Utx* KO mice (Figure 2E). These results suggest that *Utx* may play an important role in the acquisition of effector function and subsequent migration to the tumor site from dLNs.

3.2 | Decreased effector signature gene expression and increased expression of naïve or memory signature genes in *Utx* KO effector CD8⁺ T cells

Splenic naïve CD8⁺ T cells were purified from WT or *Utx* KO mice, stimulated with anti-TCR- β and anti-CD28 mAbs for 2 days, and cultured in the presence of IL-2 for another 3 days. The cells were used to analyze the role of *Utx* in CD8⁺ T cells. RNA sequencing (RNA-seq), and subsequent GO analyses of DEGs between WT and *Utx* KO mice revealed that the expression of genes related to inflammatory responses and T-cell-mediated cytotoxic activity was downregulated

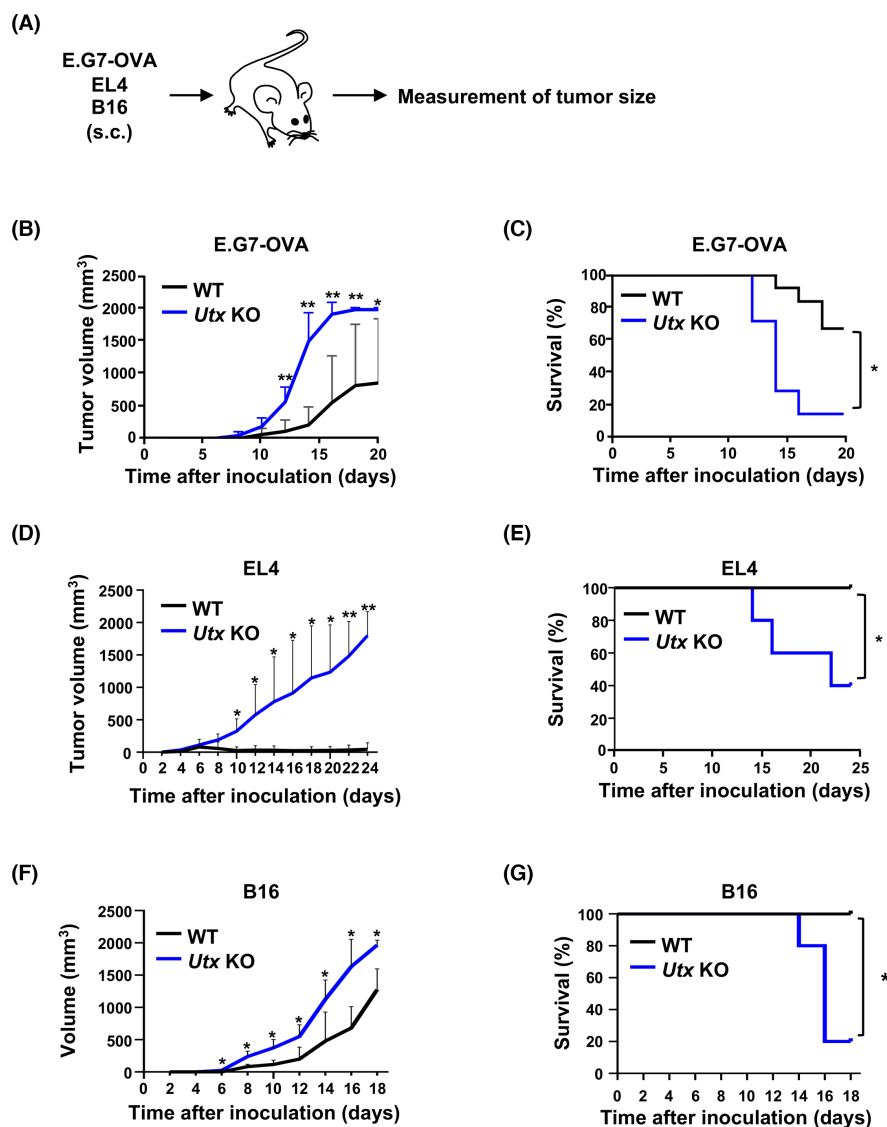


FIGURE 1 Antitumor activity was attenuated in T-cell-specific *Utx*-deficient mice. (A) Experimental layout of a tumor-bearing mouse model ($n = 7$ per group). (B) Kinetics of the tumor size measured after E.G7-OVA inoculation. (C) Kaplan–Meier survival curve of E.G7-OVA-inoculated mice. (D) Kinetics of the tumor size measured after EL4 inoculation. (E) Kaplan–Meier survival curve of EL4-inoculated mice. (F) Kinetics of the tumor size measured after B16 inoculation. (G) Kaplan–Meier survival curve of B16-inoculated mice. (B–G), C57BL/6 mice were used as WT mice and *Utx*^{fllox/fllox} CD4-Cre Tg mice were used as *Utx* KO mice. (B, D, F) Analyses with a two-tailed unpaired *t*-test (* $p < 0.05$, ** $p < 0.001$). (C, E, G) Analyses with the log-rank test (* $p < 0.05$).

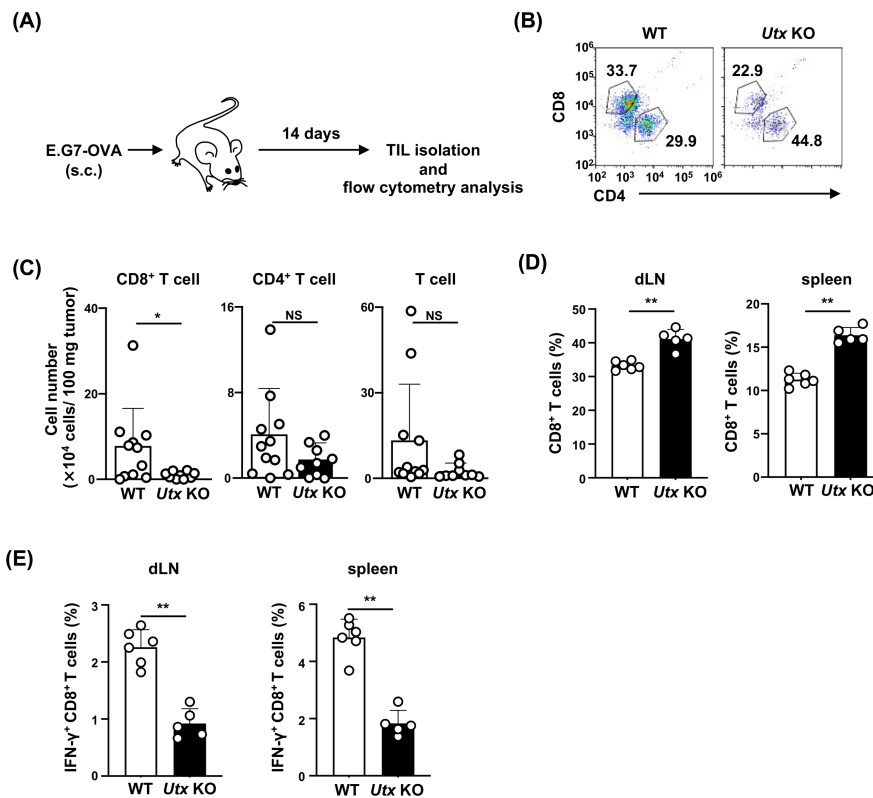


FIGURE 2 Numbers of total and IFN- γ -producing CD8⁺ TILs were decreased in T-cell-specific *Utx*-deficient mice. (A) Experimental layout for the tumor-infiltrating lymphocytes (TIL) analysis. Analyses were performed 14 days after E.G7-OVA inoculation (WT, $n = 11$ and *Utx* KO, $n = 9$ per group). (B) Percentage of CD8⁺ and CD4⁺ T cells among TILs. (C) Absolute numbers of TCR- β ⁺ T cells among CD8⁺ TILs, CD4⁺ TILs and TILs. Each point represents an individual mouse (mean \pm SD). (D, E) Analyses were performed 12 days after E.G7-OVA inoculation (WT, $n = 6$ and *Utx* KO, $n = 5$ per group). Isolated cells from dLNs and spleen in tumor-bearing mice were stimulated with PMA (10 ng/mL) plus ionomycin (500 nM) for 4 h in the presence of monensin (2 μ M). The percentage of CD8⁺ T cells among total living cells (D) and the percentage of IFN- γ -positive cells among CD8⁺ T cells (E). Each point represents an individual mouse (mean \pm SD). * $p < 0.05$, ** $p < 0.001$ (two-tailed unpaired *t*-test). C57BL/6 mice were used as WT mice, and *Utx*^{flox/flox} CD4-Cre Tg mice were used as *Utx* KO mice.

in *Utx* KO CD8⁺ T cells compared to WT CD8⁺ T cells (Figure 3A). The gene expression profiles of naïve, effector, and memory signatures in CD8⁺ T cells by a GSEA revealed that the effector signature was significantly enriched in WT mice, whereas the naïve and memory signatures were enriched in *Utx* KO mice (Figure 3B, Figure S2). Thus, naïve and memory signature genes, such as *Bach2* and *Lef1*, were found to be upregulated in *Utx* KO mice, whereas the expression of effector signature genes, such as *Ifng* and *Prf1*, was downregulated in these models (Figure 3C).

Consistent with the decreased expression of effector signature genes and the increased expression of naïve or memory signature genes in *Utx* KO CD8⁺ T cells by a comprehensive RNA-seq analysis (Figure S3A,B), qRT-PCR also showed a significantly decreased expression of *Eomes* and *Id2* (effector-related genes) and slightly decreased expression of *Tbx21* (effector-related genes) in *Utx* KO CD8⁺ T cells (Figure 4A). In sharp contrast, the expression of naïve-related and memory-related genes, such as *Bach2*, *Bcl6*, *Id3*, *Lef1*, *Sox4*, and *Tcf7*, was significantly increased in effector *Utx* KO CD8⁺ T cells compared with WT CD8⁺ T cells (Figure 4B). These results support the notion that effector differentiation is suppressed by *Utx* deficiency.

3.3 | Decreased effector functions in *Utx* KO CD8⁺ T cells

The cultured cells were then analyzed for the expression of CD62L and CD44 molecules by flow cytometry on days 4 and 5 after the initial TCR- β /CD28 mAb stimulation to assess the differentiation status of effector CD8⁺ T cells. Consistent with the RNA-seq data, the frequency of CD62L^{high}CD44^{high} effector CD8⁺ T cells in *Utx* KO cultures was significantly lower than that in WT cultures, while the frequency of CD62L^{high}CD44^{low} naïve/stem cell-like memory CD8⁺ T cells was significantly higher in *Utx* KO cultures (Figure 5A). We assessed the cytokine production ability of in vitro-stimulated *Utx* KO CD8⁺ T cells on days 4 and 5 by intracellular staining and on day 4 by an ELISA and found that the generation of IFN- γ -, IL-2-, and TNF- α producing cells was significantly lower in *Utx* KO CD8⁺ T-cell cultures than in WT CD8⁺ T-cell cultures (Figure 5B). The reduced production of IFN- γ , IL-2 and TNF- α in *Utx*-deficient effector CD8⁺ T cells was confirmed by an ELISA (Figure 5C). The mRNA expression of *Gzmb* and *Prf1* genes was also decreased in *Utx* KO CD8⁺ T cells compared with WT CD8⁺ T cells (Figure 5D).

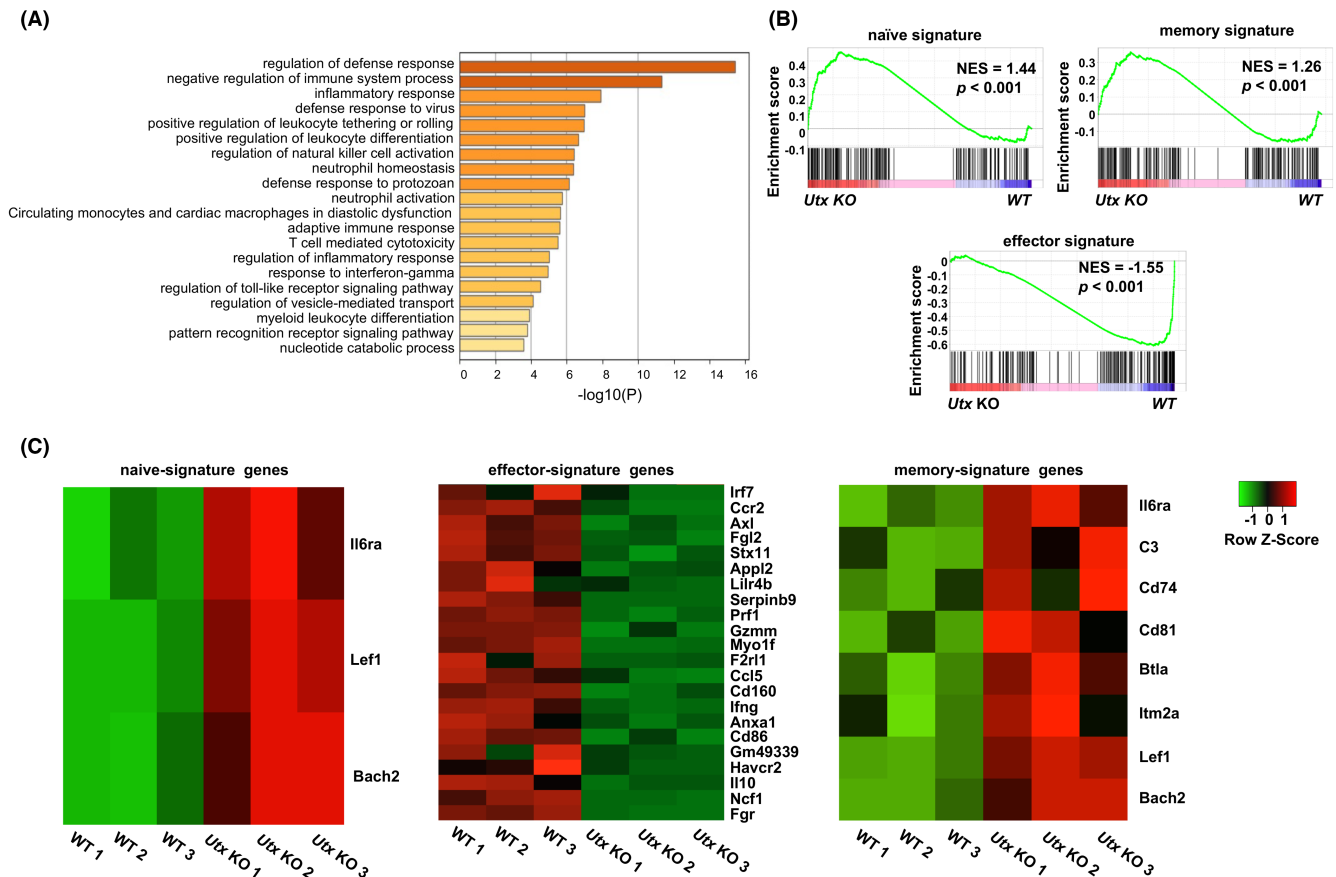


FIGURE 3 The expression of effector signature genes was reduced in *Utx* KO CD8⁺ T cells. WT and *Utx* KO naïve CD8⁺ T cells were stimulated with anti-TCR- β mAb plus anti-CD28 mAb with IL-2, and then the cells were further expanded with IL-2 for an additional 3 days. The cells were used for RNA-seq analyses ($n=3$ biological replicates). (A) The top 20 GO terms enriched for downregulated differentially expressed genes (DEGs) in *Utx* KO are shown. FC < -2 , FDR < 0.05 . (B) GSEA plots of naïve (top left), memory (top right), and effector (bottom) signature genes in WT and *Utx* KO cells. The normalized enrichment score (NES) and p -value are shown. (C) Heatmaps showing the expression status of DEGs in RNA-seq that are upregulated (FC > 2 , FDR < 0.05) in naïve signature genes (left panel) and memory signature genes (right panel) and downregulated (FC < -2 , FDR < 0.05) in effector signature genes (middle panel).

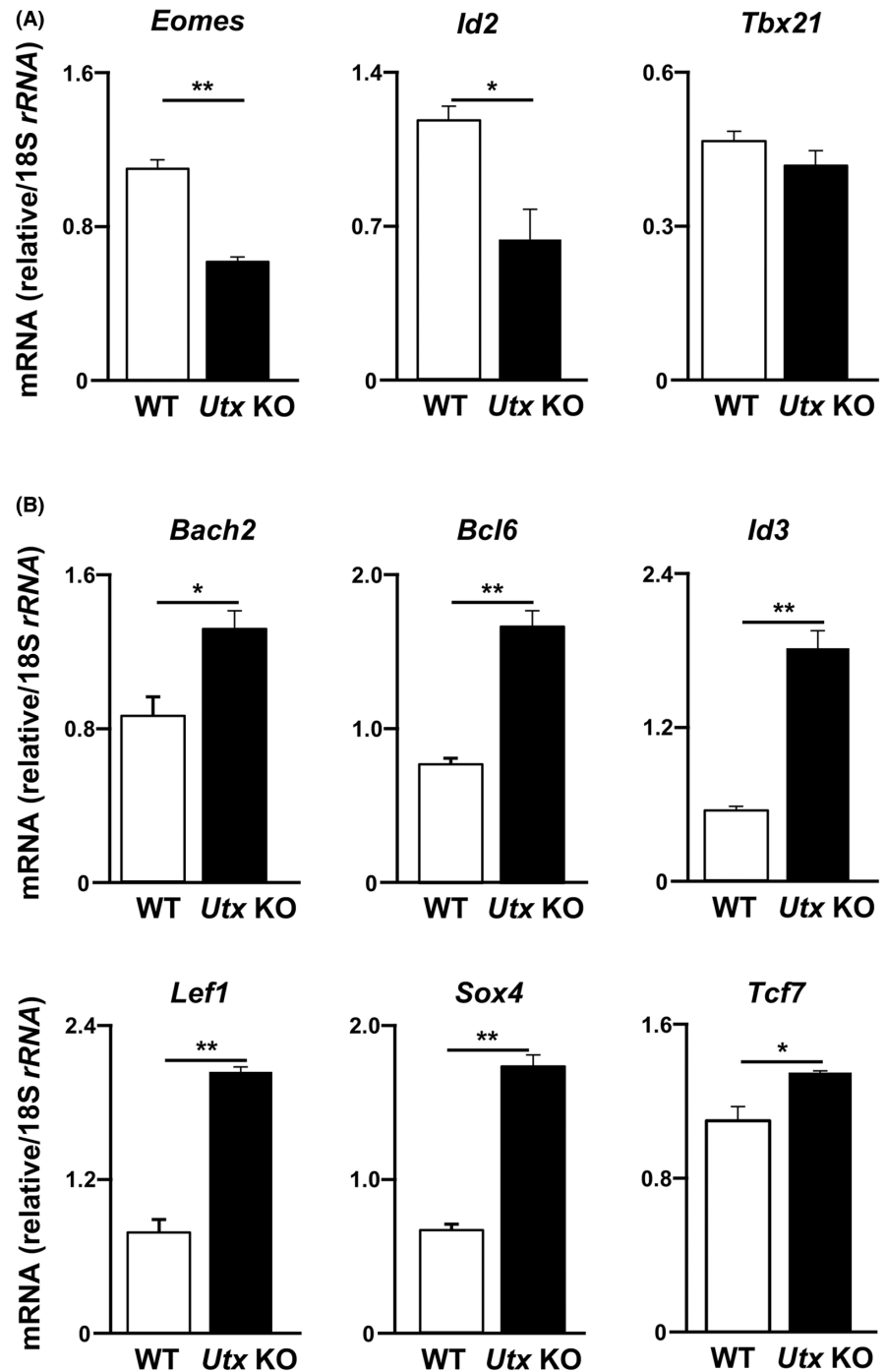
Next, we evaluated the proliferative response of *Utx* KO CD8⁺ T cells. The cell division induced by TCR- β /CD28 mAb stimulation in the presence of IL-2 on days 2 and 3s was moderately reduced in *Utx* KO CD8⁺ T cells compared with that in WT CD8⁺ T cells (Figure S4). Furthermore, we performed a killing assay to examine the antigen-specific cytotoxic activity in vitro. As shown in Figure 5E, *Utx* KO effector CD8⁺ T cells showed a significantly lower killing activity than WT CD8⁺ T cells. These results suggest that *Utx* is required for the acquisition of the full effector function in activated CD8⁺ T cells.

3.4 | Requirement for *Utx* to induce *Cxcr3* in effector CD8⁺ T cells

The result of RNA-seq results showed decreased mRNA expression of the chemokine receptors *Ccr2*, *Cxcr6*, and *Cxcr3* in *Utx* KO effector CD8⁺ T cells (Figure 6A). Among these, *Cxcr3*, a chemokine receptor critical for the migration of CD8⁺ T cells to the tumor site^{12,30–32} showed the most striking reduction in *Utx* KO effector CD8⁺ T cells. Therefore, we performed qRT-PCR to determine the

kinetics of the *Cxcr3* mRNA expression in in vitro-activated CD8⁺ T cells. The expression of *Cxcr3* mRNA in WT CD8⁺ cells was increased at 2 days after the initial TCR- β /CD28 mAb stimulation, peaked at day 3, and remained elevated until day 7 (Figure 6B). In contrast, *Utx* KO CD8⁺ T cells did not show an increase in *Cxcr3* mRNA after TCR- β /CD28 mAb stimulation (Figure 6B). The significant reduction in the cell surface expression of the *Cxcr3* protein in in vitro-cultured *Utx* KO CD8⁺ T cells was confirmed by flow cytometry (Figure 6C). In addition, *Ezh2* deficiency in in vitro-activated CD8⁺ T cells resulted in an increase in the cell surface expression of the *Cxcr3* protein (Figure 55). To confirm the decreased *Cxcr3* expression in *Utx* KO CD8⁺ T cells in vivo, we used a murine infection model of OVA-expressing *L. monocytogenes* (*Lm*-OVA) to detect OVA antigen-specific CD8⁺ T cells by MHC class I tetramers pulsed with OVA peptide (Figure 6D). The expression of *Cxcr3* on OVA-specific CD8⁺ T cells from the spleen of *Lm*-OVA-infected T-cell-specific *Utx* KO mice was decreased compared with that from infected WT mice (Figure 6E). The number of OVA-specific CD8⁺ T cells in the spleen was also significantly reduced in *Utx* KO mice (Figure 6F). The expression level of *Cxcr3* was slightly decreased in antigen-specific

FIGURE 4 The expression of naïve-related and memory-related genes was increased in *Utx* KO CD8⁺ T cells. (A, B) The mRNA expression of effector-related genes (A) and naïve/memory-related genes (B) in WT and *Utx* KO CD8⁺ T cells on day 5 after initial TCR stimulation was determined by qRT-PCR. The results are presented relative to the expression of 18s rRNA (mean ± SD, *n* = 3, technical replicates). The results (A, B) are representative of three independent experiments with similar results. **p* < 0.05, ***p* < 0.001 (two-tailed unpaired *t*-test).



and total CD8⁺ T cells in the dLNs of tumor-bearing *Utx* KO mice compared with those in WT mice (Figure S6A). Additionally, the expression of *Cxcr3* in total splenic CD8⁺ T cells was significantly decreased in *Utx* KO mice compared with WT mice (Figure S6B).

3.5 | Epigenetic regulation of *Cxcr3* by *Utx* in effector CD8⁺ T cells

Finally, we assessed whether or not *Utx* regulates the methylation status of histone H3K27 at the *Cxcr3* gene locus using a ChIP

assay (Figure S7A). As shown in Figure S7B, the methylation level of H3K27me₃ at the 5' upstream and coding regions of the *Cxcr3* gene was elevated in *Utx* KO CD8⁺ T cells compared with WT CD8⁺ T cells. The increased histone H3K27 di-methylation and tri-methylation at the intron regions of the *Cxcr3* gene (indicated red) in *Utx* KO CD8⁺ T cells was confirmed by ChIP-qPCR analysis (Figure S7C). These results implied that *Utx*-dependent demethylation of histone H3K27 was essential for the proper induction of *Cxcr3* expression in effector CD8⁺ T cells. *Utx* is required for the formation of an effector-type enhancer landscape in antigen-stimulated CD8⁺ T cells.

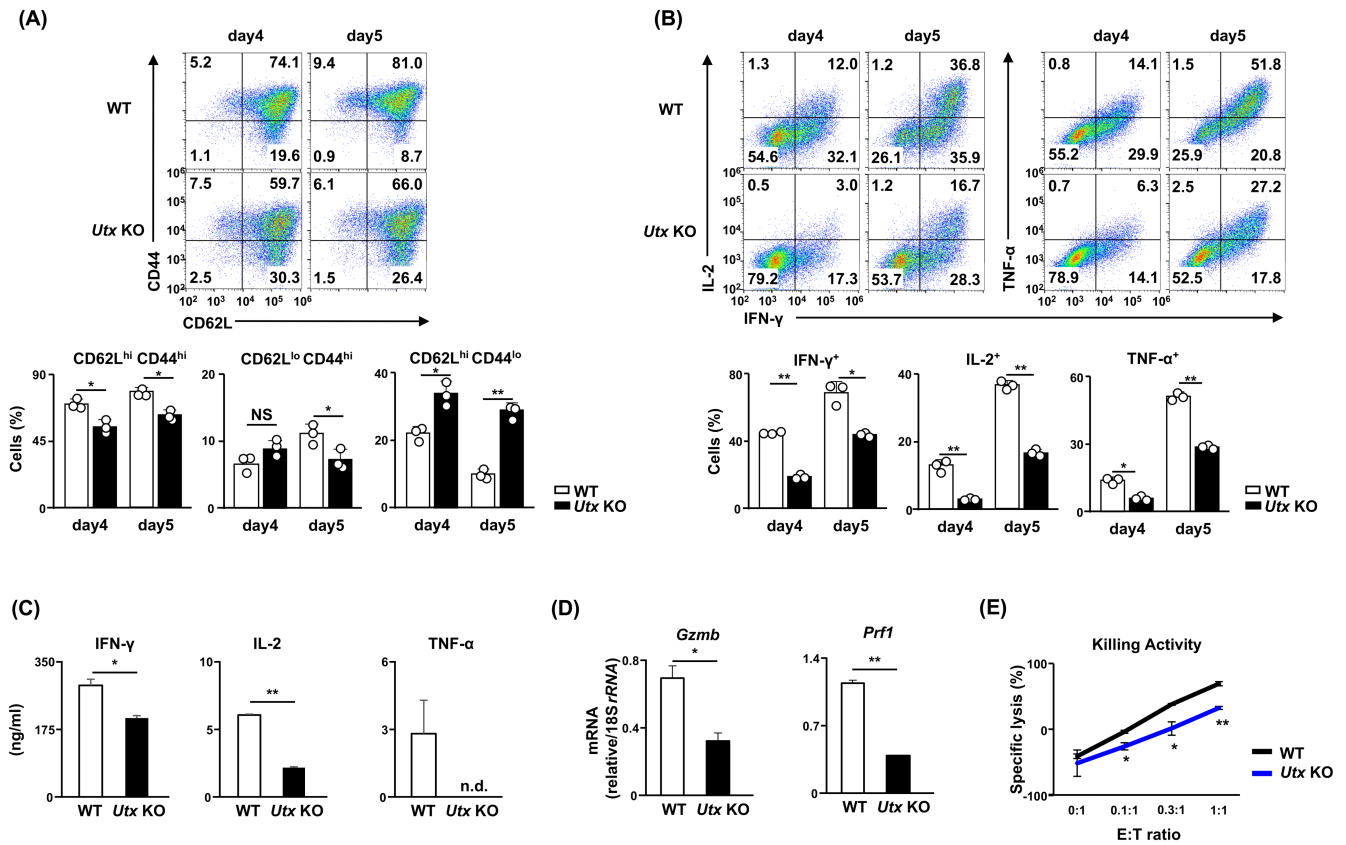


FIGURE 5 Effector CD8⁺ T-cell differentiation was decreased by Utx deficiency. (A) Representative staining profiles of CD44 and CD62L in WT and *Utx* KO CD8⁺ T cells on the indicated days (mean \pm SD, $n=3$, biological replicates). The percentages of cells are indicated in each quadrant. (B) Representative results of the intracellular staining of IFN- γ , IL-2, and TNF- α in the cells (mean \pm SD, $n=3$, biological replicates). (C) ELISA for IFN- γ , IL-2, and TNF- α in the supernatants of the cells in (A) restimulated with immobilized anti-TCR- β for 16 h (mean \pm SD, $n=3$, biological replicates). (D) The expression of *gzmb* and *prf1* genes in WT and *Utx* KO CD8⁺ T cells on day 5 was analyzed by qRT-PCR. The results are presented relative to the expression of 18s rRNA (mean \pm SD, $n=3$ technical replicates). (E) OT-1 CD8⁺ T cells were purified from the spleen of WT and *Utx* KO mice with OT-1 Tg background and then stimulated with anti-TCR- β mAb plus anti-CD28 mAb in the presence of IL-2 for 2 days. The cells were then further expanded with IL-2 for an additional 3 days. Killing activity of cultured OVA-specific OT-1 effector CD8⁺ T cells on day 5 against OVA-expressing E.G7 tumor cells as the target. The percentage of specific lysis was examined at different ratios of effector OT-1 CD8⁺ T cells (E) and target E.G7 tumor cells (T) with standard deviation ($n=3$, biological replicates). The results (A–D) are representative of three independent experiments with similar results. * $p < 0.05$, ** $p < 0.001$ (two-tailed unpaired *t*-test).

4 | DISCUSSION

Epigenetic alterations and subsequent comprehensive and coordinated changes in the gene expression determine the fate of activated CD8⁺ T cells.^{33,34} In the present study, we focused on the demethylation of histone H3K27, an inhibitory histone modification, and analyzed the effect of Utx, a histone H3K27 demethylase, on CD8⁺ T-cell differentiation and antitumor activity. We found that Utx is required for the proper induction of effector-related gene expression. As reported by Mitchell et al. using a viral infection model,³⁵ our present study showed that the loss of Utx reduced cytokine production from effector CD8⁺ T cells, including IFN- γ , TNF- α , and IL-2. In addition, the expression of perforin and granzyme B and effector-related transcription factors, such as Eomes and Id2, decreased in *Utx* KO CD8⁺ T cells. We previously reported that memory CD8⁺ T-cell formation is significantly increased in T-cell-specific *Utx* KO mice.²⁰ RNA-seq and qRT-PCR

analyses in this study also showed that the expression of naïve-related and memory-related transcription factors, including *Id3*, *Bach2*, *Sox4*, *Bcl6*, *Tcf7*, and *Lef1*, was significantly increased in *Utx*-deficient CD8⁺ T cells. These results suggest that Utx is required for the formation of an effector-type enhancer landscape in antigen-stimulated CD8⁺ T cells.

The expression of *Cxcr3*, which plays an important role in CD8⁺ T-cell migration to tumor sites,¹² is regulated by the Utx-dependent demethylation of histone H3K27. Furthermore, the mRNA expression of *Ccr2* and *Cxcr6*, chemokine receptors required for migration to inflammatory sites,^{36,37} was decreased in *Utx* KO effector CD8⁺ T cells. In sharp contrast, the expression of *Cxcr3* was upregulated in *Ezh2*-deficient effector CD8⁺ T cells. Therefore, it is likely that the balance between Utx and *Ezh2* activity controls *Cxcr3* and infiltration of CD8⁺ T cells at tumor sites and subsequent antitumor activity through the regulation of the methylation status of histone H3K27. However, previous reports have shown that the loss of *Ezh2* in T cells

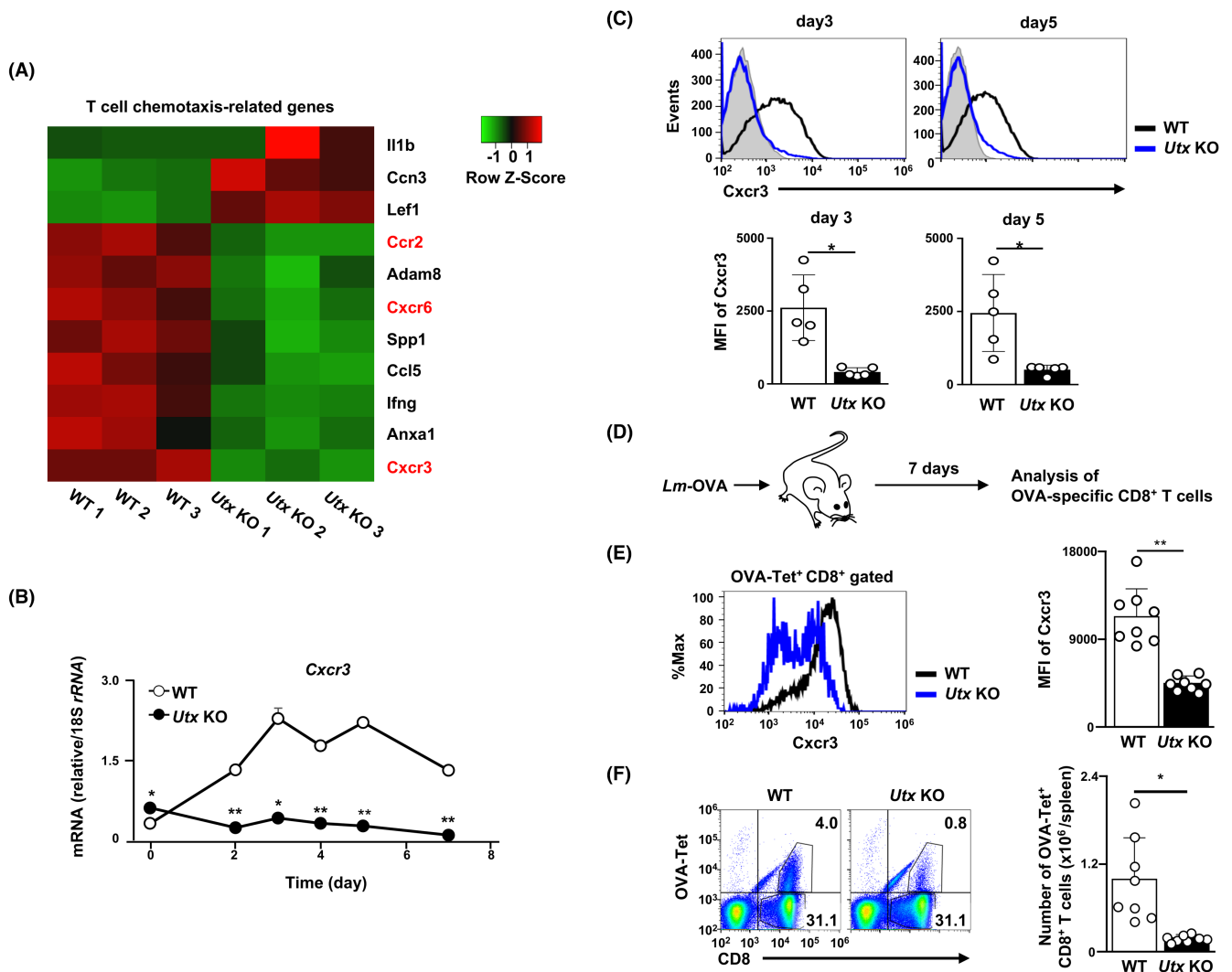


FIGURE 6 The expression of *Cxcr3* is decreased in *Utx* KO CD8⁺ T cells. WT and *Utx* KO naïve CD8⁺ T cells were stimulated with anti-TCR- β mAb plus anti-CD28 mAb with IL-2 for 2 days, and then the cells were further expanded with IL-2 for the indicated duration. (A) Heatmap showing the expression of genes involved in T-cell chemotaxis among DEGs (FC >2 or FC <-2, FDR <0.05) in RNA-seq data (Figure 3). (B) *Cxcr3* mRNA expression in WT and *Utx* KO CD8⁺ T cells was determined by qRT-PCR. The results are presented relative to the expression of 18S rRNA with the standard deviations (mean \pm SD, n = 3 technical replicates). (C) Representative surface staining profiles of *Cxcr3* in WT and *Utx* KO CD8⁺ T cells on the indicated days (upper panel). The median fluorescence intensity (MFI) of *Cxcr3* is shown (lower panel) (mean \pm SD, n = 5 biological replicates). (D) Schematic representation of the experiment using *Lm*-OVA-infected mouse models. OVA-specific CD8⁺ T cells from the spleen were analyzed on day 7 after *Lm*-OVA infection. (n = 8 per group). (E) Representative results of *Cxcr3* expression in OVA-specific (OVA-Tet⁺) CD8⁺ T cells from WT and *Utx* KO mice (mean \pm SD, n = 8). (F) Representative staining profile of OVA-specific CD8⁺ T cells (left panel) and the number of OVA-specific CD8⁺ T cells (right panel) (mean \pm SD, n = 8 per group). The result (B) is representative of at least three independent experiments with similar results. * p < 0.05, ** p < 0.001 (two-tailed unpaired t -test).

attenuates antitumor activity.^{38,39} Furthermore, it was also reported that Ezh2 is involved in the acquisition of the effector function and the survival in human T cells.³⁸ Therefore, the role of Ezh2 in antitumor immunity should be further analyzed in detail in future studies.

We have previously reported that glutaminolysis regulates the H3K27 methylation status in activated CD8⁺ T cells through the supplementation with α -ketoglutarate (α -KG).⁴⁰ α -KG regulates the enzymatic activity of JmjC family histone demethylases, including Utx.⁴¹ Nabe et al. demonstrated that CD8⁺ T cells cultured under glutamine-restricted conditions in vitro preferentially differentiated

into memory CD8⁺ T cells after adoptive transfer into naïve mice.⁴² Supplementation with α -KG antagonized the effect of glutamine restriction. Thus, the glutamine- α -KG axis determines activated CD8⁺ T-cell fate, in part through the regulation of the methylation status of histone H3K27. We showed that the regulation of histone H3K27 methylation levels by Utx controls the balance of the expression between effector T-cell-related genes and naïve or memory T-cell-related genes in the present study. In addition, we reported in a previous study that Utx suppresses the differentiation of memory CD8⁺ T cells.²⁰ These results suggest that cellular metabolism and

epigenetic enzymes, such as *Utx*, cooperatively regulate activated CD8⁺ T-cell fate.

Miller et al. reported that *Cxcr3* is a T-bet-dependent target gene and that the interaction of T-bet and *Jmjd3* is required for *Cxcr3* gene expression in Th1 cells, but they did not mention whether *Utx* is involved in the regulation of *Cxcr3* expression by T-bet.⁴³ In addition to T-bet, effector CD8⁺ T cells express *Eomes*, another T-bet protein. We demonstrated that the expression of *Eomes* was reduced by *Utx* deficiency, whereas that of *T-bet* was not. In addition, the tri-methylation level of histone H3K27 of the *Eomes* gene locus was higher in *Utx* KO effector CD8⁺ T cells than in WT CD8⁺ T cells (HN, JS, and MY unpublished observation). We speculated that *Eomes* is the predominant T-box-type transcription factor that induces *Cxcr3* expression in CD8⁺ T cells. The RNA-seq data in the present study suggested that not only *Cxcr3* but also *Cxcr6*, which is coexpressed with *Eomes* in CD8⁺ T cells and NK cells, are downregulated in *Utx* KO CD8⁺ T cells.^{44,45} *Cxcr3* and *Cxcr6* gene expression may thus be regulated by *Utx* through epigenetic regulation of *Eomes* expression.

In recent years, chimeric antigen receptor (CAR)-T-cell therapy has been developed and clinically applied for the treatment of hematologic tumors, such as leukemia, with good therapeutic results.^{46–48} If our present experimental results can be used to regulate *Cxcr3* expression and effector function in CAR-T cells, antitumor activity may be enhanced by promoting the migration of CAR-T cells to tumor sites. In addition, intervention in the gene expression profile of CAR-T cells through epigenetic and/or metabolic regulation may improve therapeutic outcomes. Furthermore, in parallel with anticancer therapy by immune checkpoint inhibition, such as via anti-PD-L1 antibodies, the promotion of T-cell migration to the tumor site by controlling chemokine receptor expression may enable more effective cancer treatment and contribute to the prognosis of cancer patients.

AUTHOR CONTRIBUTIONS

Haruna Noda, Junpei Suzuki, and Masakatsu Yamashita contributed significantly to the conception and design of this study. Haruna Noda, Junpei Suzuki, Yuko Matsuoka, and Akira Matsumoto conducted the experiments and analyzed the data. Haruna Noda drafted and revised the manuscript. Junpei Suzuki and Masakatsu Yamashita made important revisions to the manuscript. The final manuscript was read and approved by all authors.

ACKNOWLEDGMENTS

This study was supported by the Division of Medical Research Support, the Advanced Research Support Center (ADRES), Ehime University. We thank Ms. Aya Tamai for maintaining the mice.

FUNDING INFORMATION

This work was supported by JSPS KAKENHI Grant Numbers 20H03504, 22K07121, and 22K15609.

CONFLICT OF INTEREST STATEMENT

The authors declare no conflict of interest.

ETHICS STATEMENT

Approval of the research protocol by an Institutional Reviewer Board: N/A.

Informed Consent: N/A.

Registry and the Registration No. of the study/trial: N/A.

Animal Studies: The animal experiments were approved by the Ehime University Animal Experiment Committee (approval no. 05KO29-16) and conducted in accordance with the laws and regulations concerning animal experiments, animal care and keeping standards, and basic guidelines.

ORCID

Masakatsu Yamashita  <https://orcid.org/0000-0002-8975-3513>

REFERENCES

- Rosenberg SA. Progress in human tumor immunology and immunotherapy. *Nature*. 2001;411:380-384.
- Chen DS, Irving BA, Hodi FS. Molecular pathways: next-generation immunotherapy—inhibiting programmed death-ligand 1 and programmed death-1. *Clin Cancer Res*. 2012;18:6580-6587.
- Kataoka K, Shiraishi Y, Takeda Y, et al. Aberrant PD-L1 expression through 3'-UTR disruption in multiple cancers. *Nature*. 2016;534:402-406.
- Liu SV, Reck M, Mansfield AS, et al. Updated overall survival and PD-L1 subgroup analysis of patients with extensive-stage small-cell lung cancer treated with atezolizumab, carboplatin, and etoposide (IMpower133). *J Clin Oncol*. 2021;39:619-630.
- Qin S, Ren Z, Feng YH, et al. Atezolizumab plus bevacizumab versus sorafenib in the Chinese subpopulation with unresectable hepatocellular carcinoma: phase 3 randomized, open-label IMbrave150 study. *Liver Cancer*. 2021;10:296-308.
- Schmid P, Adams S, Rugo HS, et al. Atezolizumab and nab-paclitaxel in advanced triple-negative breast cancer. *N Engl J Med*. 2018;379:2108-2121.
- Chheda ZS, Sharma RK, Jala VR, Luster AD, Haribabu B. Chemoattractant receptors BLT1 and CXCR3 regulate antitumor immunity by facilitating CD8⁺ T cell migration into tumors. *J Immunol*. 2016;197:2016-2026.
- González-Martín A, Gómez L, Lustgarten J, Mira E, Mañes S. Maximal T cell-mediated antitumor responses rely upon CCR5 expression in both CD4(+) and CD8(+) T cells. *Cancer Res*. 2011;71:5455-5466.
- Lavergne E, Combadière C, Iga M, et al. Intratumoral CC chemokine ligand 5 overexpression delays tumor growth and increases tumor cell infiltration. *J Immunol*. 2004;173:3755-3762.
- Harjunpää H, Lloret Asens M, Guenther C, Fagerholm SC. Cell adhesion molecules and their roles and regulation in the immune and tumor microenvironment. *Front Immunol*. 2019;10:1078.
- Foster JG, Carter E, Kilty I, MacKenzie AB, Ward SG. Mitochondrial superoxide generation enhances P2X7R-mediated loss of cell surface CD62L on naive human CD4⁺ T lymphocytes. *J Immunol*. 2013;190:1551-1559.
- Gunderson AJ, Yamazaki T, McCarty K, et al. TGFβ suppresses CD8(+) T cell expression of CXCR3 and tumor trafficking. *Nat Commun*. 2020;11:1749.
- Kaech SM, Cui W. Transcriptional control of effector and memory CD8⁺ T cell differentiation. *Nat Rev Immunol*. 2012;12:749-761.
- Wilson CB, Makar KW, Pérez-Melgosa M. Epigenetic regulation of T cell fate and function. *J Infect Dis*. 2002;185(Suppl 1):S37-S45.
- Felsenfeld G. A brief history of epigenetics. *Cold Spring Harb Perspect Biol*. 2014;6:a018200.

16. Hu Q, Zhang X, Sun M, Jiang B, Zhang Z, Sun D. Potential epigenetic molecular regulatory networks in ocular neovascularization. *Front Genet.* 2022;13:970224.
17. Barski A, Cuddapah S, Cui K, et al. High-resolution profiling of histone methylations in the human genome. *Cell.* 2007;129:823-837.
18. Heintzman ND, Hon GC, Hawkins RD, et al. Histone modifications at human enhancers reflect global cell-type-specific gene expression. *Nature.* 2009;459:108-112.
19. Stairiker CJ, Thomas GD, Salek-Ardakani S. EZH2 as a regulator of CD8⁺ T cell fate and function. *Front Immunol.* 2020;11:593203.
20. Yamada T, Nabe S, Toriyama K, et al. Histone H3K27 demethylase negatively controls the memory formation of antigen-stimulated CD8(+) T cells. *J Immunol.* 2019;202:1088-1098.
21. Manna S, Kim JK, Baugé C, et al. Histone H3 lysine 27 demethylases Jmjd3 and Utx are required for T-cell differentiation. *Nat Commun.* 2015;6:8152.
22. Mochizuki-Kashio M, Mishima Y, Miyagi S, et al. Dependency on the polycomb gene Ezh2 distinguishes fetal from adult hematopoietic stem cells. *Blood.* 2011;118:6553-6561.
23. Hirabayashi Y, Suzuki N, Tsuboi M, et al. Polycomb limits the neurogenic competence of neural precursor cells to promote astrogenic fate transition. *Neuron.* 2009;63:600-613.
24. Kuwahara M, Yamashita M, Shinoda K, et al. The transcription factor Sox4 is a downstream target of signaling by the cytokine TGF- β and suppresses T(H)2 differentiation. *Nat Immunol.* 2012;13:778-786.
25. Zhou Y, Zhou B, Pache L, et al. Metascape provides a biologist-oriented resource for the analysis of systems-level datasets. *Nat Commun.* 2019;10:1523.
26. Babicki S, Arndt D, Marcu A, et al. Heatmapper: web-enabled heat-mapping for all. *Nucleic Acids Res.* 2016;44:W147-W153.
27. Subramanian A, Tamayo P, Mootha VK, et al. Gene set enrichment analysis: a knowledge-based approach for interpreting genome-wide expression profiles. *Proc Natl Acad Sci USA.* 2005;102:15545-15550.
28. Mootha VK, Lindgren CM, Eriksson KF, et al. PGC-1 α -responsive genes involved in oxidative phosphorylation are coordinately downregulated in human diabetes. *Nat Genet.* 2003;34:267-273.
29. Yamada T, Kanoh M, Nabe S, et al. Menin plays a critical role in the regulation of the antigen-specific CD8⁺ T cell response upon listeria infection. *J Immunol.* 2016;197:4079-4089.
30. Groom JR, Luster AD. CXCR3 in T cell function. *Exp Cell Res.* 2011;317:620-631.
31. Campanella GS, Grimm J, Manice LA, et al. Oligomerization of CXCL10 is necessary for endothelial cell presentation and *in vivo* activity. *J Immunol.* 2006;177:6991-6998.
32. Cole KE, Strick CA, Paradis TJ, et al. Interferon-inducible T cell alpha chemoattractant (I-TAC): a novel non-ELR CXC chemokine with potent activity on activated T cells through selective high affinity binding to CXCR3. *J Exp Med.* 1998;187:2009-2021.
33. Henning AN, Roychoudhuri R, Restifo NP. Epigenetic control of CD8(+) T cell differentiation. *Nat Rev Immunol.* 2018;18:340-356.
34. Crompton JG, Narayanan M, Cuddapah S, et al. Lineage relationship of CD8(+) T cell subsets is revealed by progressive changes in the epigenetic landscape. *Cell Mol Immunol.* 2016;13:502-513.
35. Mitchell JE, Lund MM, Starmer J, et al. UTX promotes CD8(+) T cell-mediated antiviral defenses but reduces T cell durability. *Cell Rep.* 2021;35:108966.
36. Mohan K, Issekutz TB. Blockade of chemokine receptor CXCR3 inhibits T cell recruitment to inflamed joints and decreases the severity of adjuvant arthritis. *J Immunol.* 2007;179:8463-8469.
37. Wehr A, Baeck C, Heymann F, et al. Chemokine receptor CXCR6-dependent hepatic NK T cell accumulation promotes inflammation and liver fibrosis. *J Immunol.* 2013;190:5226-5236.
38. Zhao E, Maj T, Kryczek I, et al. Cancer mediates effector T cell dysfunction by targeting microRNAs and EZH2 via glycolysis restriction. *Nat Immunol.* 2016;17:95-103.
39. Long H, Xiang T, Luo J, et al. The tumor microenvironment disarms CD8(+) T lymphocyte function via a miR-26a-EZH2 axis. *Oncotargets Ther.* 2016;5:e1245267.
40. Suzuki J, Yamada T, Inoue K, et al. The tumor suppressor menin prevents effector CD8 T-cell dysfunction by targeting mTORC1-dependent metabolic activation. *Nat Commun.* 2018;9:3296.
41. Kohli RM, Zhang Y. TET enzymes, TDG and the dynamics of DNA demethylation. *Nature.* 2013;502:472-479.
42. Nabe S, Yamada T, Suzuki J, et al. Reinforce the antitumor activity of CD8(+) T cells via glutamine restriction. *Cancer Sci.* 2018;109:3737-3750.
43. Miller SA, Mohn SE, Weinmann AS. Jmjd3 and UTX play a demethylase-independent role in chromatin remodeling to regulate T-box family member-dependent gene expression. *Mol Cell.* 2010;40:594-605.
44. Stegmann KA, Robertson F, Hansi N, et al. CXCR6 marks a novel subset of T-bet(lo)Eomes(hi) natural killer cells residing in human liver. *Sci Rep.* 2016;6:26157.
45. De Pelsmaecker S, Denaeghel S, Hermans L, Favoreel HW. Identification of a porcine liver Eomes(high)T-bet(low) NK cell subset that resembles human liver resident NK cells. *Front Immunol.* 2019;10:2561.
46. Porter DL, Kalos M, Zheng Z, Levine B, June C. Chimeric antigen receptor therapy for B-cell malignancies. *J Cancer.* 2011;2:331-332.
47. Porter DL, Levine BL, Kalos M, Bagg A, June CH. Chimeric antigen receptor-modified T cells in chronic lymphoid leukemia. *N Engl J Med.* 2011;365:725-733.
48. Kalos M, Levine BL, Porter DL, et al. T cells with chimeric antigen receptors have potent antitumor effects and can establish memory in patients with advanced leukemia. *Sci Transl Med.* 2011;3:95-73.

SUPPORTING INFORMATION

Additional supporting information can be found online in the Supporting Information section at the end of this article.

How to cite this article: Noda H, Suzuki J, Matsuoka Y, et al. The histone demethylase Utx controls CD8⁺ T-cell-dependent antitumor immunity via epigenetic regulation of the effector function. *Cancer Sci.* 2023;114:2787-2797. doi:[10.1111/cas.15814](https://doi.org/10.1111/cas.15814)